Effect of Char Loading on Reduction Kinetics of Cu-Based Oxygen Carriers in a Drop-Tube Fluidized Bed Reactor at Temperatures from 850° C to 1100° C: Experiment and CFD Modeling

Supporting Information

Ward A. Burgess,[*,a,b] *Nicholas C. Means,*[a,b] *Bret H. Howard,*[a] *Mark W. Smith,*[c] *Dushyant Shekhawat*[c]

[a] United States Department of Energy, National Energy Technology Laboratory, 626 Cochrans Mill Road, Pittsburgh, PA 15236, United States

[b] Leidos Research Support Team, 626 Cochrans Mill Road, PO Box 10940, Pittsburgh, Pennsylvania 15236, United States

[c] National Energy Technology Laboratory, United States Department of Energy, 3610 Collins Ferry Road, Morgantown, West Virginia 26507, United States

*Corresponding Author: E-mail: Ward.Burgess@NETL.DOE.GOV; Tel: 1-412-386-5409

A1. Mass Transfer Calculations

To obtain a well-functioning CFD model, mass generation rates for each solid and gas species must be properly calculated. The apparent reaction rate constant k_x defined in Equations S1a and S1b depends on not only the intrinsic (true) reaction rate constant k_{rx} but also depends on particle surface area S and external mass transfer coefficient k_g and effectiveness factor η. Equation S1a should be used when k_{rx} is in units of s^{-1}, and Equation S1b should be used when k_{rx} is in units of cm/s.

$$\frac{1}{k_x} = \frac{1}{k_g S} + \frac{1}{\eta k_{rx}} \tag{S1a}$$

$$\frac{1}{k_x} = \frac{1}{k_g S} + \frac{1}{\eta k_{rx} S_{BET}} \tag{S1b}$$

To calculate apparent rate constants k_4 and k_5 for coal char combustion reactions 4 and 5 in Table 5 of this paper, it is necessary to know k_g, S, η, S_{BET}, k_{r4}, and k_{r5}. Equation S2 was defined for the external mass transfer coefficient k_g from the char particles in units of cm/s.[1] External surface area S and internal pore surface area S_{BET} are determined from Tables S1 and S2, η according to Equations S4 through S7 using the values in Table S2, and k_{r4} and k_{r5} according to Table 5 in the manuscript. Then, substituting all these values into Equation S1b, the apparent rate constants k_4 and k_5 for Reactions 4 and 5 can be calculated.

$$k_g = \frac{0.75 D_0}{d_p} \frac{P_0}{P} \left(\frac{T_m}{T_0}\right)^{1.75} \tag{S2}$$

Table S1. Variables used in Equations S1 through S7.

Variable	Units	Definition
T_m	K	Mean temperature of boundary layer around particle
P	bar	Pressure
T_0	K	Reference temperature (1800 K)
P_0	bar	Reference pressure (1 bar)
D_0	cm^2/s	Diffusivity at reference T_0, P_0 (4.38 cm^2/s)
k_x	1/s	Overall rate constant for reaction *x*
k_g	cm/s	external mass transfer coefficient
k_{rx}	1/s	intrinsic reaction rate constant for reaction x
S	cm^2/cm^3	external particle surface area per unit volume ($S = 6/d_p$)
η	none	effectiveness factor for particle; accounts for mass transfer resistance because of pore diffusion rate limitations
ϕ	none	Thiele modulus
d_p	cm	Average particle diameter (0.014 cm for both char and carrier)
D_e	cm^2/s	Effective diffusivity of gas through pores of particle
r_p	cm	Mean pore radius
ϵ	none	porosity
S_{BET}	cm^2/cm^3	Pore surface area per unit volume measured by BET
T	K	Temperature of gas diffusing through pores
MW	g/mol	Molecular weight of diffusing gas
x_{char}	none	Mass fraction of char in char particles
x_{ash}	none	Mass fraction of ash in char particles

It should be noted that the average diameter of the char particles will decrease as they are consumed by chemical reaction. To account for this decrease in diameter, the value of d_P for char was multiplied by a relative diameter correction factor d_{rel}.

$$d_{rel} = \left[\frac{\frac{x_{char}}{x_{ash}}}{\left(\frac{x_{char}}{x_{ash}}\right)_0} \right]^{\frac{1}{3}} \quad \text{(S3)}$$

The effectiveness factor η is calculated as

$$\eta = \frac{3}{\phi^2}(\phi \coth \phi - 1) \quad \text{(S4)}$$

The Thiele modulus ϕ is

$$\phi = \frac{d_p}{6}\left(\frac{k_x}{D_e}\right)^{0.5} \quad \text{(S5)}$$

$$D_e = 9700\varepsilon^2 r_p \left(\frac{T}{MW}\right)^{0.5} \quad \text{(S6)}$$

In Equation S6, the effective diffusivity D_e is approximated as equal to the Knudsen diffusivity. The mean pore radius r_p is calculated with knowledge of the porosity ε and BET surface area S_{BET} of the particle. BET surface areas and porosity values for the CuO, Cu_2O and C char are given in Table S2. These values were then used in the CFD model for Reactions 1-11 as discussed in the following section.

$$r_p = \frac{2\varepsilon}{S_{BET}} \quad \text{(S7)}$$

Table S2. Values for the porosity ε, BET pore surface area S_{BET}, and mean pore radius r_p for CuO, Cu_2O, and C used in this work.

	CuO	Cu_2O	C char
ε	0.0122	0.00264	0.309
S_{BET} (cm^2/cm^3)	40000	10000	3610000
r_p (nm)	6.1	5.1	1.7

For Reactions 1-11, selected values for k_gS and ηk_r are plotted in Figure S1. In Figure S1a the rate constant $(k_gS)_{CuO}$ for external mass diffusion from CuO/Cu_2O is 2-3 orders of magnitude higher than the effective reaction rate constants ηk_{r2}, ηk_{r3}, and ηk_{r10} for Reactions 2,3

and 10; thus resistance to mass transfer because of external mass diffusion resistance can be neglected in these calculations. For all reactions considered in this section, k_{rx} values were determined from Table 5 while setting average particle diameter d_p equal to 0.014 cm. The effectiveness factor η was calculated by substituting the values from Table S2 into Equations S4-S7. For Reactions 2, 3, and 10, such calculations yielded the conclusion that in each case the effectiveness factor $\eta << 1$. Because $\eta << 1$ for Reactions 2, 3 and 10 it is concluded that each of these reactions is controlled by the rate of internal diffusion of the reacting CO gas through the pores of the CuO/Cu_2O.

From Figure S1b effective reaction rate constant ηk_9 [$k_9 = k_{9,1}P_{CO2}/(1 + k_{9,2}P_{CO2})$] for CO_2 gasification Reaction 9 is 6-7 orders of magnitude smaller than the rate constant $(k_gS)_C$ for external mass diffusion from C char. Preliminary calculations determined that, at the temperature and pressure conditions studied in this work, intrinsic reaction rate for both steam gasification Reaction 7 and CO_2 gasification Reaction 9 is sufficiently slow such that effectiveness factor η = 1. Thus it can be concluded that both of these reactions are controlled solely by the intrinsic kinetics and both external mass diffusion and internal pore diffusion can be neglected in the CFD model for Reactions 7 and 9. However, for the combustion reaction, the calculated values of $(\eta k)_4$ and $(k_gS)_C$ are similar over much of the temperature range of interest. Therefore, external diffusion, the intrinsic reaction rate constant, and pore diffusion must be considered in the CFD model to accurately model the combustion reaction kinetics.

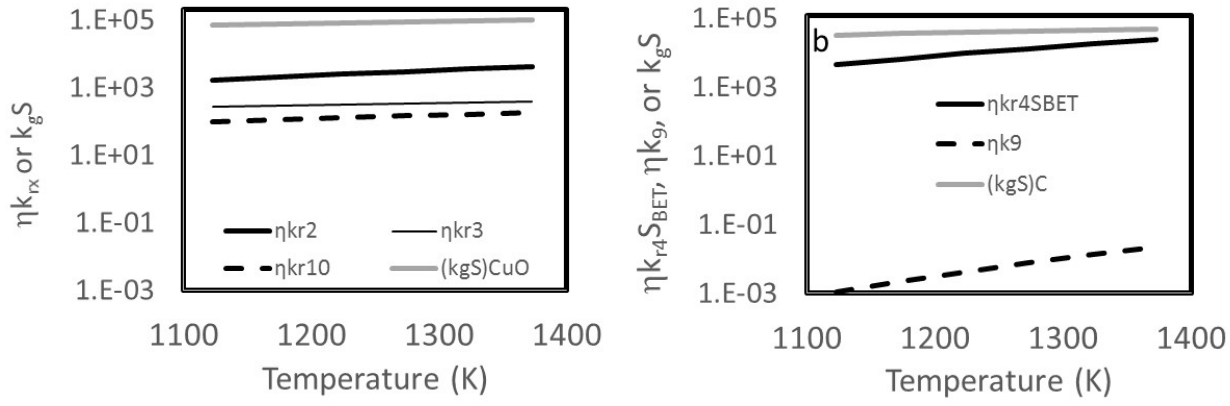

Figure S1. The net chemical reaction rate ηk_{rx} is significantly less than the external mass transfer rate k_gS for CO reduction of CuO reactions 2, 3 and 10 (Table 5 in manuscript) which involve the CuO/Cu_2O particles (a) but the effective rate constants $\eta k_4 S_{BET}$ of combustion reaction and $(k_gS)_C$ for mass transfer to/from char C particles approach parity as temperature increases (b).

A.2 Sample Calculation for Overall CuO Reduction Rate Constant $k_{ov}(T)$

To calculate k_{ov}, the full O_2, CO_2, and CO elution curve data set for a reaction must first be available. For the reduction of CuO at 900° C and C:O ratio of 0.075, the associated gas elution curves are plotted in Figure S2. At these reaction conditions almost all of the eluting gas is CO_2, with very small amounts of CO and O_2 present. The O_2 released from the reduction of CuO subsequently reacts with PRB char (denoted as $C_{(s)}$ in Figure S2) to form CO_2 and CO. Almost all the CO formed during the combustion process is oxidized to CO_2, by reaction with either O_2 or CuO. In Region 1 of Figure S2, the rate of CO_2 production is high and its concentration in the purge gas rises up to 1.5% by volume. However, at approximately 60 seconds, the CO_2 response drops rapidly and the O_2 response goes to zero. Because O_2 no longer reacts with char or CO to form CO_2 in the purge gas, the concentration of CO_2 falls sharply. At this point, it can be concluded that the CLOU reaction is nearly complete and therefore CuO composition of the carrier is negligible. The gas composition after 60 seconds in Region 2 of Figure S2 primarily arises from the undesired over-reduction of Cu_2O to Cu, which is fortunately limited by the rate of CO production from the relatively slow gasification and Cu_2O-char reactions at 900° C. Ultimately, the reaction dies and CO, CO_2 and O_2 compositions go to zero.

The X curve was calculated in the following manner. First, the volumetric flow rate of CO, CO_2, and O_2 with respect to time was calculated from the known purge gas flow rate of 1 standard L/min and the composition data shown in Figure S2. Next, these volumetric flow rates were used to calculate the molar flow rates of CO, CO_2 and O_2 with respect to time. From these molar flow rates, the total moles of oxygen $n_O(t)$ in the eluting gas and the total moles oxygen eluted $n_{O,f}$ at end of reaction were then determined. Finally, the X curve was calculated according to Equation 15 in the manuscript. It is plotted in Figure S2.

Most of the total gas elution arises before 60 seconds, as the value of X at this time is approximately 0.9. Therefore, it is assumed that the vast majority of the gas eluted is associated with the reduction of CuO and that an overall CuO reduction rate constant k_{ov} can be determined from the X data. The shrinking sphere relationship $g(X) = 1 - (1 - X)^{1/3}$ is plotted versus time up to 60 seconds to obtain an approximate, overall kinetic rate constant for the reduction of CuO. This result is plotted in Figure S3. In Figure S3, $g(X)$ begins to rise above 0 only after approximately 3 seconds, indicating that reaction just begins at about that time. The reason for this observation is that a very short time is needed for the carrier-char mixture to approach

reactor temperature after it is dropped into the reactor. Therefore, in Figure S3 the plot of *g(X)* vs *t* is not constrained to go through the origin.

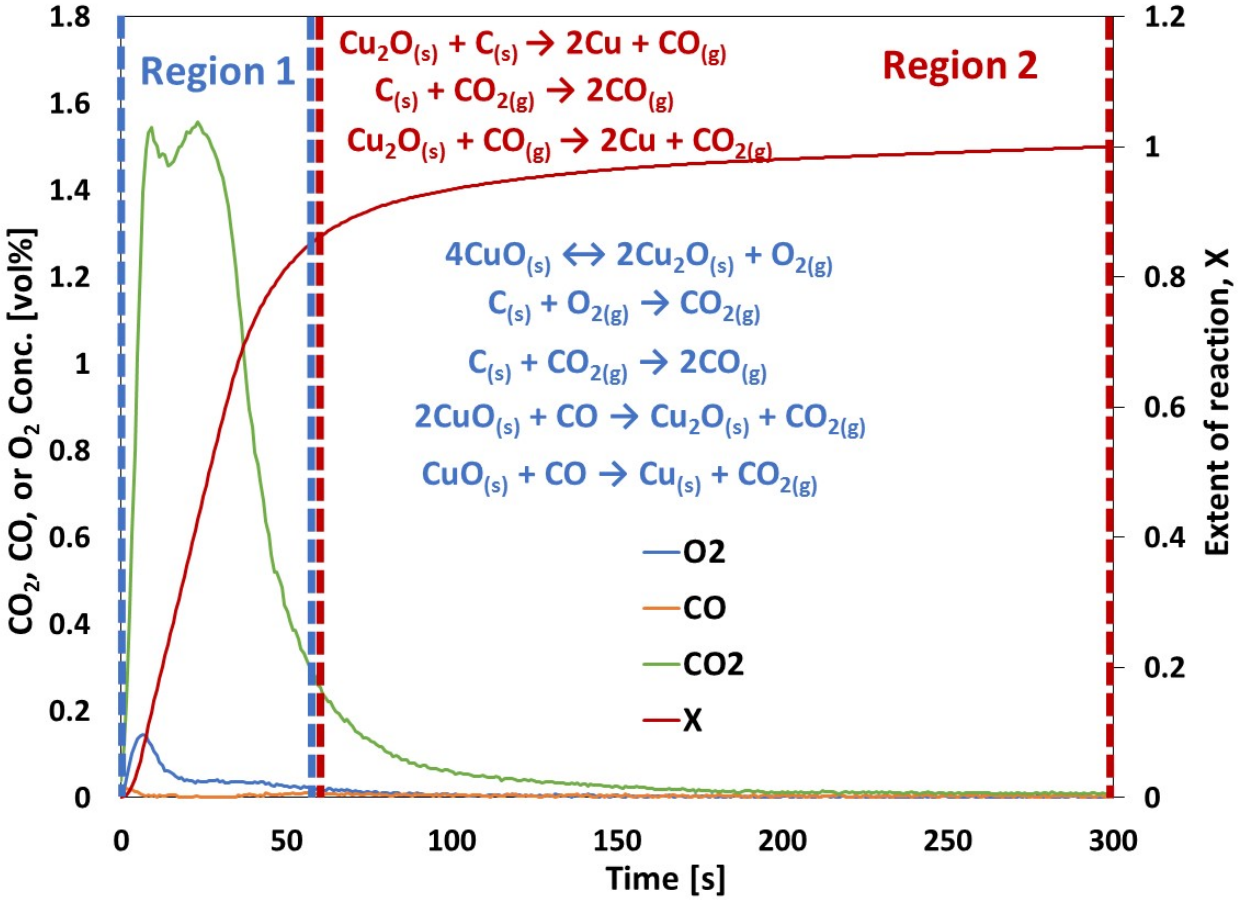

Figure S2. CO, CO_2, and O_2 gas elution curves for the reduction of CuO at 900° C with a C:O = 0.075. The extent of reaction *X* with respect to moles oxygen eluted is also plotted.

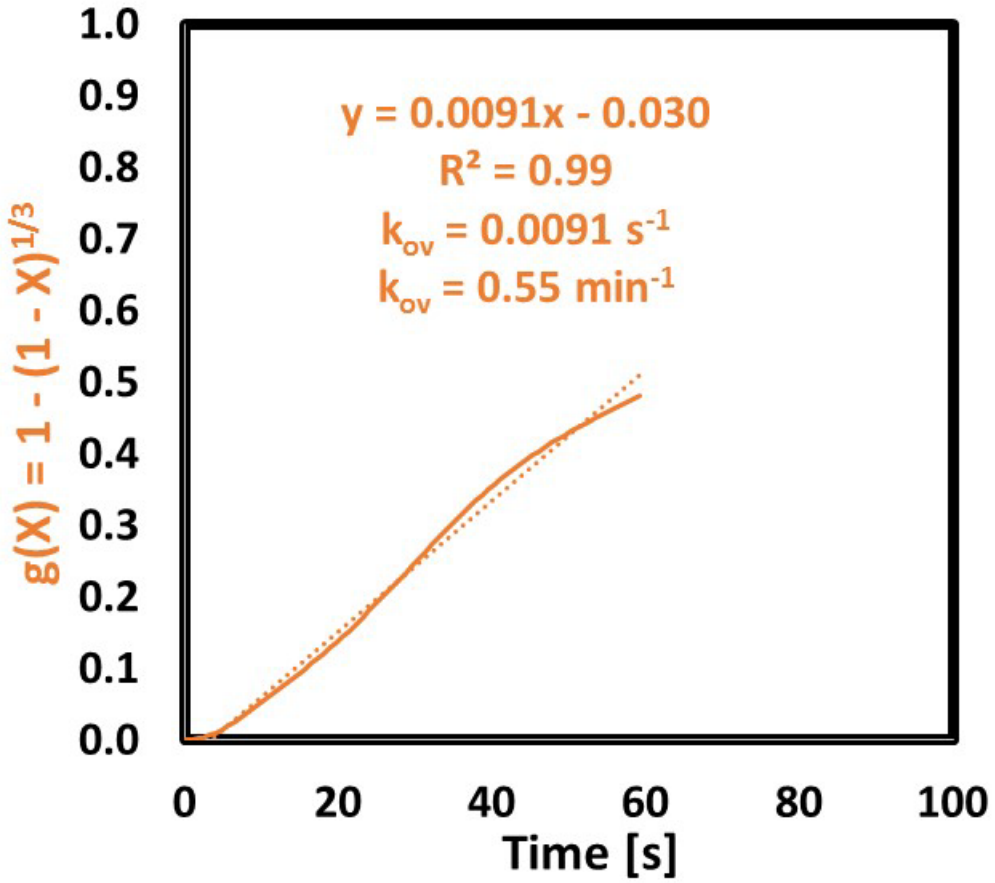

Figure S3. The overall CuO reduction rate constant k_{ov} is obtained from a plot of $g(X) = 1 - (1 - X)^{1/3}$ versus time.

A.3 Validation of Kinetic Model

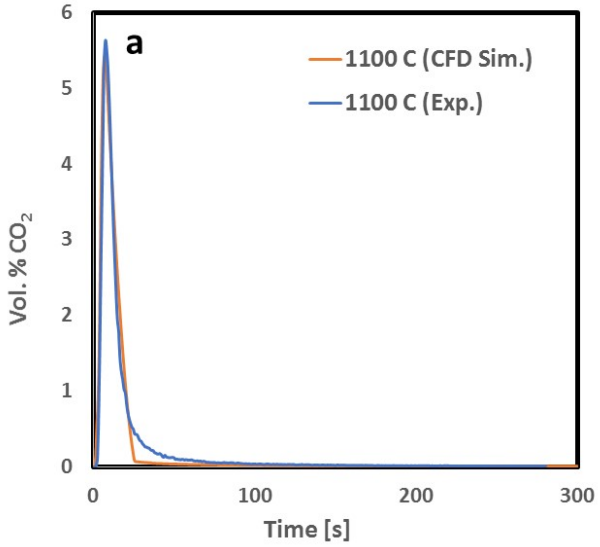

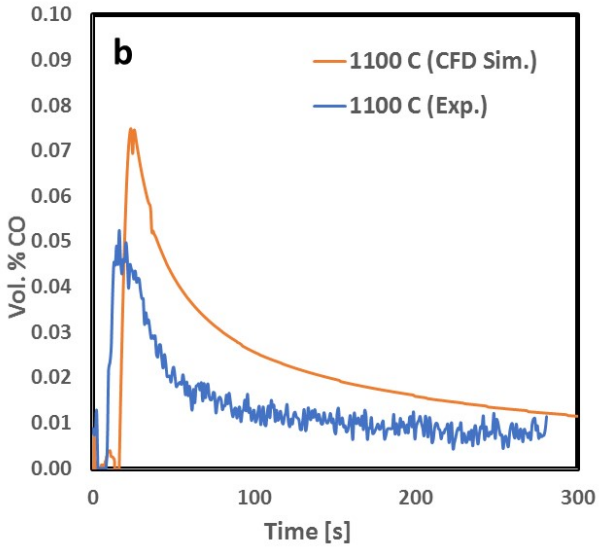

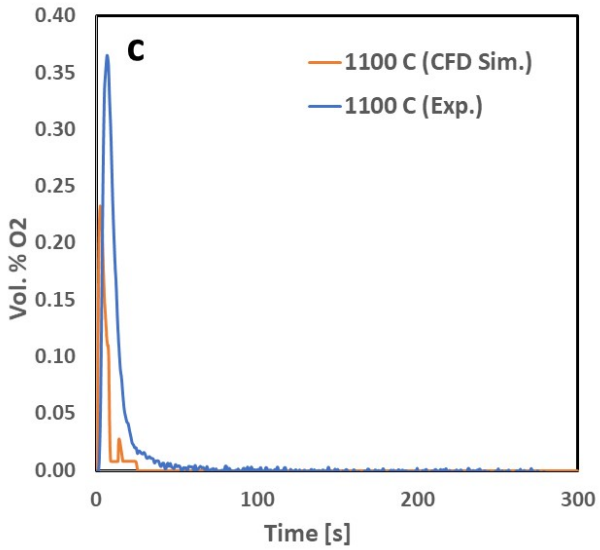

Figure S4. Comparison, for Mixed carrier, of experimentally obtained and predicted gas elution curves for (a) CO_2, (b) CO, and (c) O_2 at T = 1100° C and a C:O feed ratio of 0.075.

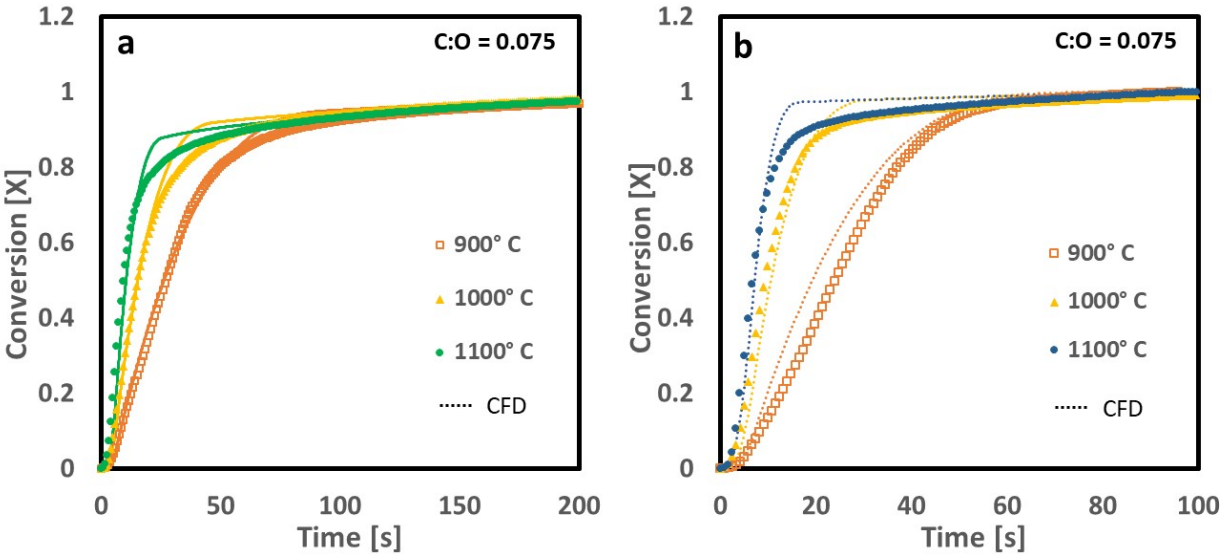

Figure S5. CFD predictions closely match *X* calculated from experimental gas elution data for (a) Mixed and (b) IWI carriers.

A4. Variation of O_2 Uncoupling, CO reduction of CuO, Combustion and Gasification Reaction Rates with Respect to C:O Ratio

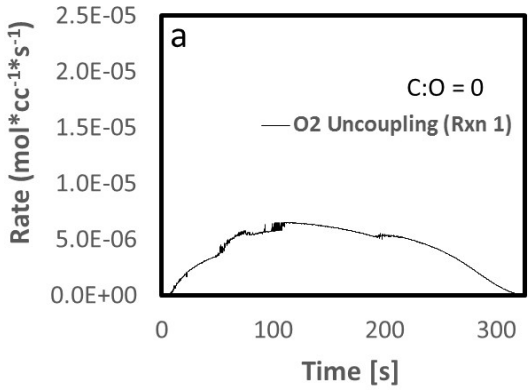

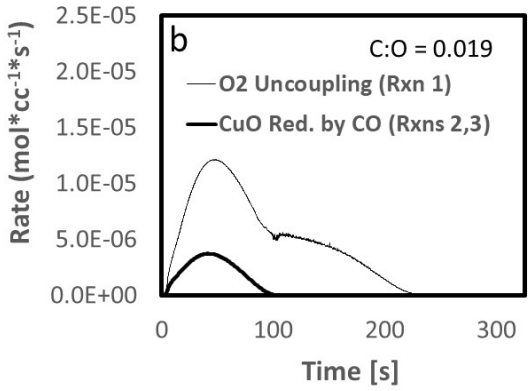

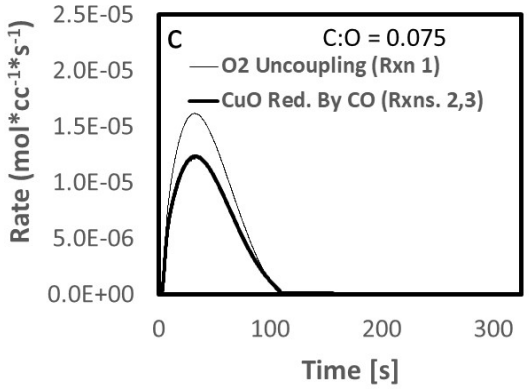

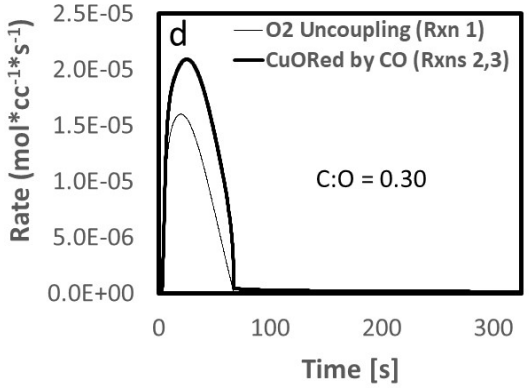

Figure S6. CFD predictions for CuO reduction rates broken down into O_2 uncoupling and reduction of CuO by CO for C:O ratio of (a) 0, (b) 0.019, (c) 0.075 and (d) 0.30.

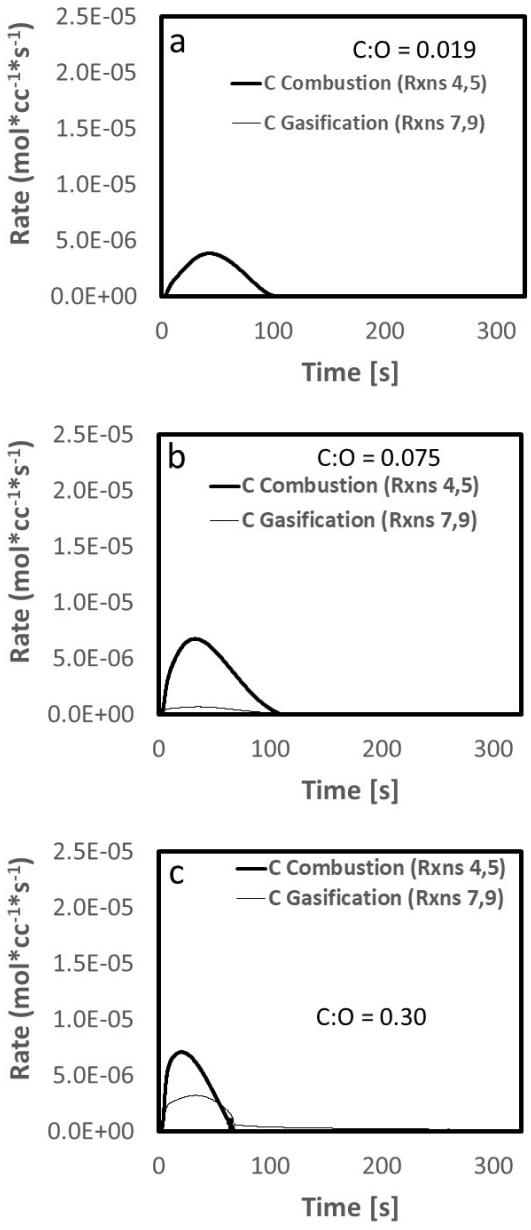

Figure S7. CFD predictions for C reaction rates broken down into combustion and gasification for C:O ratio of (a) 0.019, (b) 0.075 and (c) 0.30. The primary mode of reaction of PRB char is by combustion, but at higher C:O ratios some gasification of PRB char also occurs.

[1] Smith, I. W. The Combustion Rates of Coal Chars: A Review. Nineteenth Symposium International on Combustion/The Combustion Institute, 1982. 1045-1065.